

Journal Pre-proofs

Research Article

Imbalanced Gamma-band Functional Brain Networks of Autism Spectrum Disorders

Chen-Guang Wang, Chun Feng, Zheng-Rong Zhou, Wen-Yue Cao, Dan-Jun He, Zhong-Li Jiang, Feng Lin

PII: S0306-4522(22)00035-5
DOI: <https://doi.org/10.1016/j.neuroscience.2022.01.021>
Reference: NSC 20502

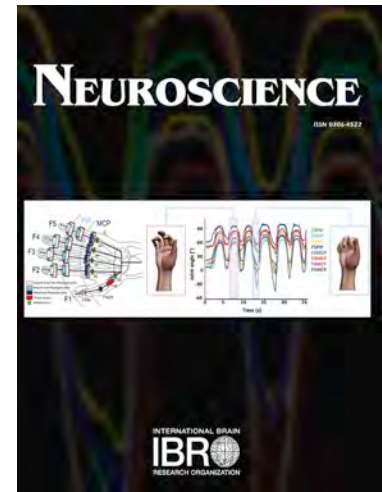
To appear in: *Neuroscience*

Received Date: 23 August 2021
Revised Date: 17 January 2022
Accepted Date: 25 January 2022

Please cite this article as: C-G. Wang, C. Feng, Z-R. Zhou, W-Y. Cao, D-J. He, Z-L. Jiang, F. Lin, Imbalanced Gamma-band Functional Brain Networks of Autism Spectrum Disorders, *Neuroscience* (2022), doi: <https://doi.org/10.1016/j.neuroscience.2022.01.021>

This is a PDF file of an article that has undergone enhancements after acceptance, such as the addition of a cover page and metadata, and formatting for readability, but it is not yet the definitive version of record. This version will undergo additional copyediting, typesetting and review before it is published in its final form, but we are providing this version to give early visibility of the article. Please note that, during the production process, errors may be discovered which could affect the content, and all legal disclaimers that apply to the journal pertain.

© 2022 The Author(s). Published by Elsevier Ltd on behalf of IBRO.



Imbalanced Gamma-band Functional Brain Networks of Autism Spectrum Disorders

Chen-Guang WANG^{1,2#}, Chun FENG^{3#}, Zheng-Rong ZHOU^{1,4}, Wen-Yue CAO¹,
Dan-Jun HE⁵, Zhong-Li JIANG^{2,6*}, Feng LIN^{2,6*}

1. School of Rehabilitation Medicine, Nanjing Medical University, Nanjing, Jiangsu, 210029, China

2. Department of Rehabilitation Medicine, The Affiliated Sir Run Run Hospital of Nanjing Medical University, Nanjing, Jiangsu, 211100, China

3. The Center of Rehabilitation Therapy, The First Rehabilitation Hospital of Shanghai, Rehabilitation Hospital Affiliated to Tongji University, Shanghai, 200090, China

4. Funing Grace Rehabilitation Hospital, Yancheng, Jiangsu, 224400, China

5. Department of Clinical Psychology, The First Affiliated Hospital of Nanjing Medical University, Nanjing, Jiangsu, 210029, China

6. Department of Rehabilitation Medicine, The First Affiliated Hospital of Nanjing Medical University, Nanjing, Jiangsu, 210029, China

These two authors contributed equally to this work.

* Co-corresponding authors:

Zhong-Li JIANG, jiangzhongli@njmu.edu.cn;

Feng LIN, peterduus@njmu.edu.cn

Abstract:

Resting gamma-band brain networks are known as an inhibitory component in functional brain networks. Although autism spectrum disorder (ASD) is considered as with imbalanced brain networks, the inhibitory component remains not fully explored. The study reported 10 children with ASD and 10 typically-developing (TD) controls. The power spectral density analysis of the gamma-band signal in the cerebral cortex was performed at the source level. The normalized phase transfer entropy values (nPTEs) were calculated to construct brain connectivity. Gamma-band activity of the ASD group was lower than the TD children. The significantly inhibited brain regions were mainly distributed in the bilateral frontal and temporal lobes. Connectivity analysis showed alterations in the connections from key nodes of the social brain network. The behavior assessments in the ASD group revealed a significantly positive correlation between the total score of Childhood Autism Rating Scale and the regional nPTEs of the right transverse temporal gyrus. Our results provide strong evidence that the gamma-band brain networks of ASD children have a lower level of brain activities and different distribution of information flows. Clinical meanings of such imbalances of both activity and connectivity were also worthy of further explorations.

Keywords: autism spectrum disorder (ASD); resting-state; gamma-band; magnetoencephalogram; brain networks

INTRODUCTION

Autism spectrum disorder (ASD) is a developmental neural disorder defined by abnormal social behavior and deficits in communication, repetitive behaviors, and restricted interests (Mostafavi & Gaitanis, 2020; Berenguer et al., 2020; American Psychiatric Association, 2013). There is a trending up the incidence of ASD among Asian kids despite about 0.36% nowadays (Qiu et al., 2020). ASD has become a non-negligible risk factor affecting the physical and mental health of children and adults. Although vast

numbers of studies have been investigated, the etiology and pathogenesis of ASD remain unclear.

Most electroencephalogram (EEG) studies suggest that there are abnormalities in children with ASD, especially in the gamma-band (Rojas & Wilson, 2014). Brain activity in the gamma-band is associated with the function of gamma-aminobutyric acid (GABA) neurons, that is, it represents the inhibitory neurotransmitter system (McNally & McCarley, 2016). The current explanation of the pathogenesis of ASD is predominantly based on the excitation-inhibition imbalance theory of signal processing in the brain (Sohal & Rubenstein, 2019). In terms of the activity level of the brain regions, van Diessen et al. reported a significant increase at the activity level of resting gamma-band among children with ASD (van Diessen et al., 2015). Meanwhile, Cornew et al. also found the same phenomena at the anterior temporal lobe, posterior frontal lobe, and occipital lobe (Cornew et al., 2012). In contrast, Sheikhan et al. reported a significant reduction in bilateral frontal gamma-band activity (Sheikhan et al., 2009, 2012). Considering the inter-regional connectivity, Shou et al. and Ye et al. observed excessive connectivity in the bilateral frontal lobe, left parietal lobe, left temporal lobe, and subcutaneous region in the resting state gamma-band (Shou et al., 2018; Ye et al., 2014). Lajiness-O'Neill et al. found reduced connections in the frontal and parietal gamma-band (Lajiness-O'Neill et al., 2018). Thus, researchers still have not achieved consensus regarding brain activity and connectivity in the gamma-band.

In recent years, brain functional network modeling has achieved significant attention. Its combination with graph theory has further promoted the research of brain networks (Hämäläinen et al., 2020; Yeh et al., 2020), which is also widely used in ASD. The brain region is considered as a node and the brain activity level is the node features. Activity synchronization or transduction among brain regions is represented as connectivity. The application of a brain function network can quantitatively analyze the physiological and pathological mechanisms of brain function activities from multiple perspectives such as

local relationships and global structure. The network paradigm illustrates a new perspective of the imbalance theory, including the in-site signal processing of individual regions and the interactive information signaling among different regions. The stability of brain network is the premise of complex cognitive function, which is largely determined by the balance of excitatory and inhibitory networks (Gray & Robinson, 2009; Menon, 2013). Dynamic GABAergic-astrocyte communication is regarded as the neurophysiological basis for inhibitory network connectivity (Mederos & Perea, 2019). In ASD, excitation-inhibition imbalance has been observed in functional brain networks (Ajram et al., 2017; Zikopoulos & Barbas, 2013; Heinze et al., 2021). Since gamma-band is linked to the function of GABA neurons, the imbalance should be obvious in gamma-band networks as well. Thus, we hypothesize that the two factors are disturbed in children with ASD, involving the reduced brain activity in gamma-band and different distribution patterns of information flow. That is, the activity of the inhibitory system is suppressed, and the signaling of inhibitory information is reallocated in the information flow networks of the brain with ASD.

To support the hypothesis, this study collected resting-state data based on MEG scanning for ASD and TD children. Regional activity and inter-regional connectivity were individually calculated as two measurements of power spectral density (PSD) and regional normalized PTEs (rnPTEs) at the signal source level. Based on the two measurements, information flow networks were constructed for comparison between the ASD and TD groups.

EXPERIMENTAL PROCEDURES

Subjects

We adopted a convenience sample of children with ASD from Funing Grace Rehabilitation Hospital in Yancheng, Jiangsu Province, China. We followed the maximum variation sampling strategy for the small sample size (Patton, 2014). It applies

the following logic: any common patterns that emerge from great variation are of particular interest and value in capturing the core experiences and central, shared dimensions of a setting or phenomenon. The eligibility criteria are listed as follows based on the previous study (Barahona-Corrêa et al., 2018; Osório & Brunoni, 2018): (1) diagnosed with ASD (in line with the "Diagnostic and Statistical Manual of Mental Disorders" 5th Edition (DSM-V) standards) at least two times based on the psychological education assessment of children with autism (Psychoeducational Profile-Third Edition, PEP-3) in the 12 months before enrollment evaluation record; (2) 7-12 years old; (3) the Child Autism Assessment Scale (CARS) greater than 30 points (Dawkins et al., 2016; Magyar & Pandolfi, 2007) or the Autism Behavior Scale (ABC) is greater than 60 points (Yousefi et al., 2015); (4) the development/adaptation of the communication items and behavior items in the PEP-3 composite score is moderate or severe; (5) right-handedness by Chinese handedness questionnaire (LI, 1983). The exclusion criteria: (1) children with attention deficit hyperactivity disorder (ADHD), speech development delay, or apraxia. (2) visual or visuospatial deficits. (3) hearing impairments. (4) mental disorders (including but not limited to depression, mental retardation, history of psychotropic drug use, etc.), epilepsy and brain injury, etc. (5) metal implanted in the body. Children with ASD usually experienced ADHD, speech development delay, and apraxia of speech. Therefore, the enrollment requirements for children without relevant previous medical history are determined by a team of clinical psychology, child development, and rehabilitation professionals. The control group consisted of 7-12 years old and right-handed TD children with no history of neurological or psychiatric diseases. Those children also have no contraindication for MEG examination.

This study was approved by the Ethics Committee of the Affiliated Sir Run Run Hospital of Nanjing Medical University (IRB# No.2019-SR-004). Informed consent was obtained orally from children and written from their legal guardian before the experiment.

Data collection

We utilized the 275-channel CTF full-head MEG system (Canada VSM Medical Technology Company) at the Nanjing Brain Hospital affiliated to Nanjing Medical University. The subjects were asked to remain as still as possible and open their eyes to focus on the black cross on a white screen in front of them. The screen is 42 cm long and 32 cm wide. The center of the screen is 35 to 45 cm away from the subject. The horizontal and vertical viewing angles of the screen sequentially are 3-4° and 1-2°. Each subject's signal was recorded for 300 seconds with a 1200Hz sampling rate and 0.03-100Hz bandpass filtering. We noted subjects' head positions before and after the experiment and excluded any movements more than 1.0cm.

Data processing

The analysis pipeline is shown in Fig. 1. MEG signals were processed by Brainstorm (Tadel et al., 2019), including 50Hz notch filtering and 0.3Hz high-pass filtering. Signal-space projection (Gross et al., 2013) and independent component analysis were used to detect artifacts of saccades, winks, and heartbeats. We selected a continuous 100-second artifact-free signal of each participant. Dynamic statistical parametric mapping was performed for source reconstruction (Dale et al., 2000). The source file for each subject was projected onto the USCBrain atlas (Joshi et al., 2017).

For each subject, the activity of the gamma-band was analyzed by the power spectral density (PSD) based on the Welch method (Solomon, 1991). We chose a 4-second window length, 50% time overlap, and 30-59Hz gamma-band (Datko et al., 2016). The surface of cerebral cortex is masked by 15000 vertices (default value), which represents the cortex envelope (Niso et al., 2019). They were also the number of electric dipoles that we used to model the activity of the brain. The USCBrain atlas divided the cerebral cortex into 130 regions of interest (ROIs) with 65 ones on each hemisphere based on the anatomy. Abbreviations and names of ROIs are exhibited in *Table S1*. According to their

spatial position, all vertices were partitioned into 130 ROIs. To reduce data volume, the source intensity of each ROI was derived by averaging signals of its vertices. A map of power spectral density with 130 ROIs was obtained for each subject.

The connectivity of the gamma-band was calculated by the normalized phase transfer entropy (nPTE) depending on the ROI signals for each subject. As a measure of information theory, the transfer entropy describes the information transfer between time series. The information flow can be quantified by the phase transfer entropy (PTE) between time series based on the phase information (Lobier et al., 2014). We adopted the nPTE to reduce biases, i.e., the effect of having extremely small PTE values in situations when there is no actual information flow (Engels et al., 2017). If the nPTE from A ROI to B ROI is greater than 0, the information flows from A to B. If the nPTE from A to B is less than 0, the information points from B to A. Each ROI (number = 130) owns 129 nPTE values. Every value denotes the information streams from this ROI to another ROI. The average of 129 nPTE values is the regional nPTE (rnPTE, ranging from -0.5 to 0.5) that measures the average degree of information exchange from the ROI to the whole brain. Thus, each ROI is named as receivers (rnPTEs<0) or drivers (rnPTEs>0) depending on the rnPTE value.

The 130 ROIs were divided into three functional systems: (1) higher order cognitive system; (2) medial default mode system; (3) sensory and association system (Muldoon et al., 2016). Brain region abbreviations and corresponding functional system are exhibited in *Table S1*.

Activity Statistical analysis

In the first step, z-score testing was employed to compare the power values of 130 ROIs in the gamma-band between the ASD group and the TD group (Pagnotta et al., 2015). The z-value test is as follows: mean value and standard deviation of gamma-band power of each ROI in the TD group and the ASD group are calculated. Two matrices are

obtained respectively (in the form of 130ROIs×1 frequency band). The z-value is calculated by the following expression:

$$Z_i = \frac{P_i - Mean_i^c}{SD_i^c} .$$

The i represents the ROI serial number, the P_i is on behalf of the i -th ROI's gamma-band PSD value, the *means* and SD^C separately represent the mean and standard deviation of the control group (Huang et al., 2012). The false discovery rate (FDR) method was applied to correct the multiple comparisons (Benjamini & Hochberg, 1995). With a threshold of $|z| = 3.52$, the FDR reaches the significance level of $p=0.05$.

The second step was the permutation T-tests with 10,000 randomizations, using the following approach: (1) Observed t values: to calculate the Student's t value for each ROI between ASD group and TD group; (2) Permuted t values: to permute the between-group assignments of PSD value for two groups, and the t values were recalculated; (3) Repeating: To obtain 10,000 permutations for each ROI by repeating the second step. (4) The observed t values were tested against the distribution of permuted t values with $\alpha=0.05$. The differences were considered as significant only when both FDR with $|z| \geq 3.52$ and permutation T-test with $p < 0.05$. The effect sizes (ES) were calculated using the Hedge's g . According to Cohen, ES from 0.2-0.49 were considered small, from 0.5 to 0.79 were considered moderate and those equal or larger than 0.8 were considered large (Cohen, 2013; Turner Herbert M. & Bernard Robert M., 2006). The significantly different z-scores were tagged onto the brain atlas for visualization and interpretation.

Connectivity Statistical analysis

Based on the mPTEs, directed graphs were sequentially established for ASD and TD groups. The direction of a link denotes that information transfers from one terminal to another. The directed links are called arcs. The absolute values of mPTEs are the weights of arcs. In graph theory, the unweighted degree of a node is the number of links it holds.

The weighted degree of a node is the weighted number of links. In this study, the weighted input degree signifies the strength of information flow an ROI receiving from other regions. The weighted output degree indicates the intensity of information flow the ROI spreading to other regions (Rubinov & Sporns, 2010). Permutation T-tests with 10,000 randomizations were decided to compare nPTEs of 130 ROIs between ASD and TD groups. The Spearman coefficients between nPTEs and CARS total score, ABC total score, and PEP-3 total score for each ROI were successively calculated. P values of correlation coefficients were corrected by the FDR ($\alpha=0.05$). ES were calculated using the Hedge's *g*, as well. The above statistical issues were accomplished with the analysis of the Brainstorm and Python3.7.

RESULTS

Behavior assessments upon enrollment

Twelve ASD and ten TD children participated in the study. Two ASD subjects were removed because of too much MEG artifact. There was no significant difference in age and gender between the two groups ($p<0.05$). See Table 1 and Fig. 2 for specific demographic characteristics.

Activity comparisons

As displayed in Fig. 3, the whole brain activity in the TD group was uneven. The ASD group consistently presented low activity, and the brain activity in the ASD group was lower than that in the TD group.

Compared with the TD group, the gamma-band of the ASD group manifested remarkably inhibited ROIs and no significantly activated ROIs. The brain regions with important inhibition mostly distributed in the bilateral frontal lobe and bilateral temporal lobe. A small amount is allocated in the bilateral insular lobe, bilateral limbic system,

bilateral parietal lobe, and bilateral occipital lobe. For each statistical result, the corresponding degree of freedom (df) was 18. See Fig. 4 and Table 2 for details.

The post-hoc power analysis for activity statistical tests (GPower version 3.1.9) showed that the sample size in our experiment yields a power of 85.6% and the lowest effect size of -1.43 at a significance level of 0.05 (two-sided). (Lenth, 2007)

Information flow Comparisons

Four ROIs in the ASD group showed significantly higher mPTEs than those in the TD group, including left anterior orbito-frontal gyrus (df=18, $t=0.002$, $p=0.017$, Hedge's $g=1.17$), left lateral orbitofrontal gyrus (df=18, $t=0.003$, $p=0.018$, Hedge's $g=1.14$), left temporal pole (df=18, $t=0.002$, $p=0.008$, Hedge's $g=1.25$), and left lateral frontal transverse gyrus (df=18, $t=0.002$, $p=0.039$, Hedge's $g=0.93$). This suggested that the ASD group had more information outflows with fewer information inflows at these brain areas. In addition, the mPTEs of 3 ROIs in the ASD group were significantly lower than those in the TD group, including anterior left angular gyrus (df=18, $t=-0.003$, $p=0.025$, Hedge's $g=-1.04$), anterior left inferior occipital gyrus (df=18, $t=-0.002$, $p=0.018$, Hedge's $g=-1.15$), and left parahippocampal gyrus (df=18, $t=-0.002$, $p=0.018$, Hedge's $g=-1.16$). This suggested that the ASD group had more information flows into these areas with less information flowing out. See Fig. 5A for the specific ROIs. Comparison of mPTEs between two groups was revealed in Fig. 5B.

Correlation of connectivity with ABC, CARS, and PEP-3

After FDR correction, the mPTEs of 130 ROIs in the ASD group had no significant correlation with the total score of ABC and PEP-3. There was a significantly positive correlation between mPTEs and CARS total score of the right Heschl's gyrus, i.e., transverse temporal gyrus. See Fig. 6 for the correlation curve and coefficient.

DISCUSSION

Various theories have pushed forward the investigations concerning the mechanism of ASD, including Theory of Mind (Baron-Cohen, 2000), Central coherence Theory (Happé, 2021) and Executive function Theory (Pellicano, 2012), and excitation-inhibition balance (E-I balance) (Sohal & Rubenstein, 2019). Each of these theories has its advantages in explaining the clinical symptoms of ASD (Bottema-Beutel et al., 2019). Among them, the theory of E-I balance has achieved more attention in the last two decades. The potential reason is that this theory supports a unified explanation for the internal mechanism and external symptoms of ASD (Howell & Smith, 2019; Sohal & Rubenstein, 2019). According to this theory, the activities of excitatory neurons and inhibitory neurons maintain the temporal and spatial balance. The balanced situation of two types of neurons determines the brain functioning. Inhibitory neurons, known as GABA neurons, have functional deficits in ASD persons, leading to weakening of the inhibitory function of the cerebral cortex and disrupting the excitation-inhibition balance. Thus, it manifests as reduced efficiency of information processing (Sohal & Rubenstein, 2019). Series of clinical symptoms will be amplified when children with less ability to process tasks are faced with overwhelming information. Activity of GABA neurons is characterized by the EEG signal in the gamma-band. Meanwhile, the decrease in the intensity of the gamma-band activity represents the inhibition of the activities of GABA neurons, i.e., the relatively overactive of the excitation component in the brain with ASD (McNally & McCarley, 2016). MEG signals provide two types of data for supporting this theory. One is attribute data, i.e., activities at specific ROIs. In this study, we used PSD to define the intensity of the brain activity. The other is relational data, i.e., functional connectivity between different ROIs. This study concerned on the information exchange between brain areas by using rnPTEs. Based on the theory of E-I balance, we hypothesize that children with ASD will demonstrate abnormal activity and information connectivity in the resting gamma-band. This is manifested in the comparison with the control group.

We found less activity of gamma band in children with ASD and an imbalance in the distribution of information connections in their brain.

Intensity of regional activity

This study compared the MEG signals between 10 children with ASD and 10 TD peers in the resting state with their eyes open. The results suggest that the brain activity of the gamma-band in children with ASD was significantly lower than that in the TD group (Fig. 3 and 4). Sheikhan et al. (2009, 2012) analyzed the signals of resting state among children with ASD at the source level using EEG 10-20 system. They found excessive inhibition in the bilateral prefrontal lobe and right temporal lobe. We subdivided the brain area into 130 ROIs and also found significant suppression of the bilateral prefrontal and right temporal lobes. Additionally, we realized the diminished activity in the entire cerebral cortex, which is largely in the bilateral prefrontal and bilateral temporal lobes, as well as slight amount in the bilateral insulae, bilateral parietal lobes, bilateral limbic systems and bilateral occipital lobes (Table 2). The insula comprises social and non-social cognitive processes, which involves the emotional expression, empathy, decision-making, self-management, and verbal communication (Uddin et al., 2017). Bolling et al. (2011) suggested low activity of bilateral insulas in ASD children in the face of social rejection and depression. Nomi et al. (2019) explored the changes in the activities of the insula in the perception and imitation tasks in ASD patients. They summarized that the lower activities of the right anterior insula were associated with social cognitive impairment. Ogawa further investigated that in the subvocalization task, the activities of the right anterior insula of ASD children were crucially related to the degree of social behavior disorders (Ogawa et al., 2019).

The prefrontal lobe and cingulate gyrus are part of the working memory network in the frontal cortex. This network primarily incorporates the prefrontal cortex, motor cortex, cingulate gyrus and parietal lobe as the neural basis of higher cognitive information and

memory processing (Barendse et al., 2013). Barendse noticed that the children with ASD have reduced information transmission ability in resting state and 1-back tasks in the working memory network. Children with ASD can compensate for working memory ability through general intelligence (Barendse et al., 2018). After a 2-year longitudinal study in an ASD group, Vogan et al. detected that with the increased age and cognitive load, the working memory network presented progressive impairments (Vogan et al., 2019). In this study, we also found significant gamma-band inhibition at the bilateral prefrontal lobes and bilateral cingulate gyri. It is speculated that an imbalance in the resting frontal and parietal working memory network in the ASD group will be unveiled. The results implied that less activity of the inhibitory system in brain areas related to social behaviors (such as the prefrontal lobe and insula) which cause a relative increase in the excitatory system. Thus, the abnormal signal processing was detected in the brain area. The signal processing is also considered a whole-brain collaboration. Future research should further attempt to discover whether the information flow is imbalanced between brain regions.

Intensity of information flow

After comparing the rnPTEs of ROIs among two groups, we identified that four ROIs in the ASD group had significantly increased information outflow. Moreover, three ROIs in the ASD group had significantly increased information inflow (Fig. 5). These brain regions are responsible for the decision-making, auditory attention, semantic processing, facial processing and memory (Boylan et al., 2015; Fatahi et al., 2020; Karanian & Slotnick, 2017; Michalka et al., 2015; Schneider et al., 2018; Uono et al., 2017)(**Table S2**). These changes provided evidence for the hypothesis that information flows are unevenly distributed in the brain of children with ASD. It has been reported that the brain networks of ASD children have reduced efficiency, broken integrity, and overloaded information (Alaerts et al., 2015; Müller & Fishman, 2018). In our study, the two of the three ROIs with more inflows were in the sensory and association system (Fig.

5B), suggesting that brain of ASD call for more processing resources to deal with sensory information. A report on neuro-network modeling described that children with ASD tend to be obsessed with trivial features of environment (Lanillos et al., 2020). They usually have redundant inhibitory connections and oversensitive feelings. The ROIs with significantly increased information outflow were mainly in the higher cognitive system, except for the left lateral frontal gyrus (Fig. 5B). This change may be a manifestation of information processing compensation in the higher cognitive system after the reduction in upper limit of ASD cognitive load. Therefore, it can be inferred from the E-I balance theory that other systems, such as sensory, are relatively enhanced in children with ASD, while the higher cognitive system is relatively weak. From the perspective of resting state as a state of task preparation, such unbalance of excitation suppression may lead to information overload and information processing disorder in task state. As a result, children with ASD usually exist with the cognitive deficits and social integration impairment.

Correlation between information flow and CARS score

We further explored associations between rnPTEs and clinical and behavioural phenotypes. CARS score was significantly positive correlated with right Heschl's gyrus rnPTEs in the sensory and association system. An increased outflow of information from the right Heschl's gyrus demonstrates more severe clinical symptoms. Right Heschl's gyrus takes part in auditory information processing (Zoellner et al., 2019). At present, no other relevant experiments have explained this correlation. We hypothesized that increased outflow information from the right Heschl's gyrus predicted decompensation of cortical information outflow distribution. This increase means that the higher cognitive system is no longer effective as driver to power the entire brain, but instead, other parts of the system, such as the sensory, are responsible for powering. This compensatory model may not be adequate. Therefore, children with ASD manifest serious clinical symptoms. However, further research is required to confirm the relationship.

Limitations

There are five challenges for our research: (1) It is important to note that we make conclusions based on the small sample size. Although we have adopted suitable statistical methods, our experimental results may still suffer from bias because of the heterogeneity of ASD children. The number of subjects will be expanded in the future and the age will be stratified; (2) IQ matching was not adopted in the control group. The biggest part of reason is that lack of gamma-band cerebral cortex activity standard and a brain network expectation model among children with the same age. Grouping factors for the control group could be added to continue refining the research results; (3) We included children who could cooperate with MEG detection, which might introduce the bias in this study; (4) Physical development was not matched. The maximum variation sampling for a small sample size does not require accurate matching of all factors. Moreover, Toscano et al. reported that the weight and BMI (Body Mass Index) of ASD children were lower than that TD children of the same age (Toscano et al., 2019); (5) Our results are limited to the gamma-band in the resting state, which does not directly reflect the overall activity of the brain. In the future, task-state gamma-band analysis can be supplemented. Meanwhile, further investigations should examine the effects of subjects' state (open or closed eyes), signal acquisition methods (EEG or MEG), and analysis methods (sensor level or signal source level) on the results.

We found the excessive suppression of brain activity at the gamma-band level in children with ASD through the trace analysis of MEG signals. At the same time, there were differences in brain network between TD and ASD children in the aspect of the distribution and intensity of the information flow at the gamma-band region. Therefore, children with ASD have an excitation-inhibition imbalance at the activity level as well as information exchanging.

Author contributions: Dr. Feng LIN and Prof. Zhong-Li JIANG designed the protocol. Chen-Guang WANG recruited subjects, performed the analysis, generated the images, and wrote the manuscript with Chun Feng. Zheng-Rong ZHOU, Wen-Yue CAO and Dan-Jun HE recruited subjects. Dr. Feng LIN also supervised the entire study, proofread the manuscript, and contributed to the research concept.

Compliance with Ethical Standards: Informed written consent was obtained from the patient for publication of this report and any accompanying images.

Acknowledge: This study is subproject of a non-invasive intervention for brain regulation study among children with ASD. We appreciate Dr. Amanda Ferland, for her professional suggestions and kind assistance with language improvements.

Disclosure: The authors report no disclosures on competing financial interests.

Funding : This work was supported by the The Affiliated Sir Run Run Hospital of Nanjing Medical University [grant numbers YFZDXK02-7].

Potential conflicts of interest: The authors declare no conflicts of interest.

Reference

- Ajram, L. A., Horder, J., Mendez, M. A., Galanopoulos, A., Brennan, L. P., Wichers, R. H., Robertson, D. M., Murphy, C. M., Zinkstok, J., Ivin, G., Heasman, M., Meek, D., Tricklebank, M. D., Barker, G. J., Lythgoe, D. J., Edden, R. A. E., Williams, S. C., Murphy, D. G. M., & McAlonan, G. M. (2017). Shifting brain inhibitory balance and connectivity of the prefrontal cortex of adults with autism spectrum disorder. *Translational Psychiatry*, 7(5), e1137–e1137. <https://doi.org/10.1038/tp.2017.104>
- Alaerts, K., Geerlings, F., Herremans, L., Swinnen, S. P., Verhoeven, J., Sunaert, S., & Wenderoth, N. (2015). Functional Organization of the Action Observation Network in Autism: A Graph Theory Approach. *PLOS ONE*, 10(8), e0137020. <https://doi.org/10.1371/journal.pone.0137020>
- American Psychiatric Association. (2013). *Diagnostic and statistical manual of mental disorders: DSM-5*. Arlington, VA.
- Barahona-Corrêa, J. B., Velosa, A., Chainho, A., Lopes, R., & Oliveira-Maia, A. J. (2018). Repetitive Transcranial Magnetic Stimulation for Treatment of Autism Spectrum Disorder: A Systematic Review and Meta-Analysis. *Frontiers in Integrative Neuroscience*, 12, 27. <https://doi.org/10.3389/fnint.2018.00027>
- Barendse, E. M., Hendriks, M. P., Jansen, J. F., Backes, W. H., Hofman, P. A., Thoonen, G., Kessels, R. P., & Aldenkamp, A. P. (2013). Working memory deficits in high-functioning adolescents with autism spectrum disorders: Neuropsychological and neuroimaging correlates. *Journal of Neurodevelopmental Disorders*, 5(1). <https://doi.org/10.1186/1866-1955-5-14>

- Barendse, E. M., Schreuder, L. J., Thoonen, G., Hendriks, M. P. H., Kessels, R. P. C., Backes, W. H., Aldenkamp, A. P., & Jansen, J. F. A. (2018). Working memory network alterations in high-functioning adolescents with an autism spectrum disorder: FMRI correlates for memory in ASD. *Psychiatry and Clinical Neurosciences*, 72(2), 73–83. <https://doi.org/10.1111/pcn.12602>
- Baron-Cohen, S. (2000). Theory of mind and autism: A review. *International Review of Research in Mental Retardation*, 23, 169–184. [https://doi.org/10.1016/S0074-7750\(00\)80010-5](https://doi.org/10.1016/S0074-7750(00)80010-5)
- Benjamini, Y., & Hochberg, Y. (1995). Controlling the False Discovery Rate: A Practical and Powerful Approach to Multiple Testing. *Journal of the Royal Statistical Society. Series B (Methodological)*, 57(1), 289–300. <https://doi.org/10.1111/j.2517-6161.1995.tb02031.x>
- Berenguer, C., Baixauli, I., Gómez, S., Andrés, M. de E. P., & De Stasio, S. (2020). Exploring the Impact of Augmented Reality in Children and Adolescents with Autism Spectrum Disorder: A Systematic Review. *International Journal of Environmental Research and Public Health*, 17(17), 6143. <https://doi.org/10.3390/ijerph17176143>
- Bolling, D. Z., Pitskel, N. B., Deen, B., Crowley, M. J., Mayes, L. C., & Pelphrey, K. A. (2011). Development of neural systems for processing social exclusion from childhood to adolescence: Neural systems for processing social exclusion. *Developmental Science*, 14(6), 1431–1444. <https://doi.org/10.1111/j.1467-7687.2011.01087.x>
- Bottema-Beutel, K., Kim, S. Y., & Crowley, S. (2019). A systematic review and meta-regression analysis of social functioning correlates in autism and typical development: Bottema-Beutel

- et al./Social functioning meta-analysis. *Autism Research*, 12(2), 152–175.
<https://doi.org/10.1002/aur.2055>
- Boylan, C., Trueswell, J. C., & Thompson-Schill, S. L. (2015). Compositionality and the angular gyrus: A multi-voxel similarity analysis of the semantic composition of nouns and verbs. *Neuropsychologia*, 78, 130–141. <https://doi.org/10.1016/j.neuropsychologia.2015.10.007>
- Cohen, J. (2013). *Statistical power analysis for the behavioral sciences*. Academic press.
- Cornew, L., Roberts, T. P. L., Blaskey, L., & Edgar, J. C. (2012). Resting-State Oscillatory Activity in Autism Spectrum Disorders. *Journal of Autism and Developmental Disorders*, 42(9), 1884–1894. <https://doi.org/10.1007/s10803-011-1431-6>
- Dale, A. M., Liu, A. K., Fischl, B. R., Buckner, R. L., Belliveau, J. W., & Lewine, J. D. (2000). Dynamic statistical parametric mapping: Combining fMRI and MEG for high-resolution imaging of cortical activity. *Neuron*, 26, 55–67.
[https://doi.org/doi:10.1016/S0896-6273\(00\)81138-1](https://doi.org/doi:10.1016/S0896-6273(00)81138-1)
- Datko, M., Gougelet, R., Huang, M.-X., & Pineda, J. A. (2016). Resting State Functional Connectivity MRI among Spectral MEG Current Sources in Children on the Autism Spectrum. *Frontiers in Neuroscience*, 10, 258. <https://doi.org/10.3389/fnins.2016.00258>
- Dawkins, T., Meyer, A. T., & Van Bourgondien, M. E. (2016). The Relationship Between the Childhood Autism Rating Scale: Second Edition and Clinical Diagnosis Utilizing the DSM-IV-TR and the DSM-5. *Journal of Autism and Developmental Disorders*, 46(10), 3361–3368. <https://doi.org/10.1007/s10803-016-2860-z>

- Fatahi, Z., Ghorbani, A., Ismail Zibaii, M., & Haghparast, A. (2020). Neural synchronization between the anterior cingulate and orbitofrontal cortices during effort-based decision making. *Neurobiology of Learning and Memory*, 175, 107320. <https://doi.org/10.1016/j.nlm.2020.107320>
- Gray, R. T., & Robinson, P. A. (2009). Stability of random brain networks with excitatory and inhibitory connections. *Advances in Machine Learning and Computational Intelligence*, 72(7), 1849–1858. <https://doi.org/10.1016/j.neucom.2008.06.001>
- Gross, J., Baillet, S., Barnes, G. R., Henson, R. N., Hillebrand, A., Jensen, O., Jerbi, K., Litvak, V., Maess, B., Oostenveld, R., & others. (2013). Good practice for conducting and reporting MEG research. *NeuroImage*, 65, 349–363. <https://doi.org/10.1016/J.NEUROIMAGE.2012.10.001>
- Hämäläinen, M., Huang, M., & Bowyer, S. M. (2020). Magnetoencephalography Signal Processing, Forward Modeling, Inverse Source Imaging, and Coherence Analysis. *Neuroimaging Clinics of North America*, 30(2), 125–143. <https://doi.org/10.1016/j.nic.2020.02.001>
- Happé, F. (2021). Weak Central Coherence. In F. R. Volkmar (Ed.), *Encyclopedia of Autism Spectrum Disorders*. Springer International Publishing. https://doi.org/10.1007/978-3-319-91280-6_1744
- Heinze, K., Barron, H. C., Howes, E. K., Ramaswami, M., & Broome, M. R. (2021). Impaired inhibitory processing: A new therapeutic target for autism and psychosis? *The British Journal of Psychiatry*, 218(6), 295–298. Cambridge Core. <https://doi.org/10.1192/bjp.2020.163>

- Howell, B. W., & Smith, K. M. (2019). Synaptic structural protein dysfunction leads to altered excitation inhibition ratios in models of autism spectrum disorder. *Pharmacological Research*, *139*, 207–214. <https://doi.org/10.1016/j.phrs.2018.11.019>
- Huang, M.-X., Nichols, S., Robb, A., Angeles, A., Drake, A., Holland, M., Asmussen, S., D'Andrea, J., Chun, W., Levy, M., Cui, L., Song, T., Baker, D. G., Hammer, P., McLay, R., Theilmann, R. J., Coimbra, R., Diwakar, M., Boyd, C., ... Lee, R. R. (2012). An automatic MEG low-frequency source imaging approach for detecting injuries in mild and moderate TBI patients with blast and non-blast causes. *NeuroImage*, *61*(4), 1067–1082. <https://doi.org/10.1016/j.neuroimage.2012.04.029>
- Joshi, A. A., Choi, S., Sonkar, G., Chong, M., Gonzalez-Martinez, J., Nair, D., Shattuck, D. W., Damasio, H., & Leahy, R. M. (2017). *A whole brain atlas with sub-parcellation of cortical gyri using resting fMRI[C]*//*Medical imaging 2017: Image processing. International Society for Optics and Photonics, 2017*, (M. A. Styner & E. D. Angelini, Eds.; Vol. 10133, p. 101330O). <https://doi.org/10.1117/12.2254681>
- Karanian, J. M., & Slotnick, S. D. (2017). False memory for context and true memory for context similarly activate the parahippocampal cortex. *Cortex*, *91*, 79–88. <https://doi.org/10.1016/j.cortex.2017.02.007>
- Lajiness-O'Neill, R., Brennan, J. R., Moran, J. E., Richard, A. E., Flores, A.-M., Swick, C., Goodcase, R., Andersen, T., McFarlane, K., Rusiniak, K., Kovelman, I., Wagley, N., Ugolini, M., Albright, J., & Bowyer, S. M. (2018). Patterns of altered neural synchrony in the default mode network in autism spectrum disorder revealed with magnetoencephalography (MEG):

- Relationship to clinical symptomatology: Altered neural synchrony in ASD. *Autism Research*, 11(3), 434–449. <https://doi.org/10.1002/aur.1908>
- Lanillos, P., Oliva, D., Philippsen, A., Yamashita, Y., Nagai, Y., & Cheng, G. (2020). A review on neural network models of schizophrenia and autism spectrum disorder. *Neural Networks*, 122, 338–363. <https://doi.org/10.1016/j.neunet.2019.10.014>
- Lenth, R. V. (2007). Post hoc power: Tables and commentary. *Iowa City: Department of Statistics and Actuarial Science, University of Iowa*, 1–13.
- LI, X.-T. (1983). Handedness distribution in Chinese population (In Chinese). *Acta Psychologica Sinica*, 15(3), 268–275. <https://doi.org/CNKI:SUN:XLXB.0.1983-03-004>
- Magyar, C. I., & Pandolfi, V. (2007). Factor Structure Evaluation of the Childhood Autism Rating Scale. *Journal of Autism and Developmental Disorders*, 37(9), 1787–1794. <https://doi.org/10.1007/s10803-006-0313-9>
- McNally, J. M., & McCarley, R. W. (2016). Gamma band oscillations: A key to understanding schizophrenia symptoms and neural circuit abnormalities. *Current Opinion in Psychiatry*, 29(3), 202–210. <https://doi.org/10.1097/YCO.0000000000000244>
- Mederos, S., & Perea, G. (2019). GABAergic-astrocyte signaling: A refinement of inhibitory brain networks. *Glia*, 67(10), 1842–1851. <https://doi.org/10.1002/glia.23644>
- Menon, V. (2013). Developmental pathways to functional brain networks: Emerging principles. *Trends in Cognitive Sciences*, 17(12), 627–640. <https://doi.org/10.1016/j.tics.2013.09.015>
- Michalka, S. W., Kong, L., Rosen, M. L., Shinn-Cunningham, B. G., & Somers, D. C. (2015). Short-Term Memory for Space and Time Flexibly Recruit Complementary Sensory-Biased

- Frontal Lobe Attention Networks. *Neuron*, 87(4), 882–892.
<https://doi.org/10.1016/j.neuron.2015.07.028>
- Mostafavi, M., & Gaitanis, J. (2020). Autism Spectrum Disorder and Medical Cannabis: Review and Clinical Experience. *Seminars in Pediatric Neurology*, 35, 100833.
<https://doi.org/10.1016/j.spen.2020.100833>
- Muldoon, S. F., Pasqualetti, F., Gu, S., Cieslak, M., Grafton, S. T., Vettel, J. M., & Bassett, D. S. (2016). Stimulation-Based Control of Dynamic Brain Networks. *PLOS Computational Biology*, 12(9), e1005076. <https://doi.org/10.1371/journal.pcbi.1005076>
- Müller, R.-A., & Fishman, I. (2018). Brain Connectivity and Neuroimaging of Social Networks in Autism. *Trends in Cognitive Sciences*, 22(12), 1103–1116.
<https://doi.org/10.1016/j.tics.2018.09.008>
- Niso, G., Tadel, F., Bock, E., Cousineau, M., Santos, A., & Baillet, S. (2019). Brainstorm Pipeline Analysis of Resting-State Data From the Open MEG Archive. *Frontiers in Neuroscience*, 13, 284. <https://doi.org/10.3389/fnins.2019.00284>
- Nomi, J. S., Molnar-Szakacs, I., & Uddin, L. Q. (2019). Insular function in autism: Update and future directions in neuroimaging and interventions. *Progress in Neuro-Psychopharmacology and Biological Psychiatry*, 89, 412–426. <https://doi.org/10.1016/j.pnpbp.2018.10.015>
- Ogawa, R., Kagitani-Shimono, K., Matsuzaki, J., Tanigawa, J., Hanaie, R., Yamamoto, T., Tominaga, K., Hirata, M., Mohri, I., & Taniike, M. (2019). Abnormal cortical activation during silent reading in adolescents with autism spectrum disorder. *Brain and Development*, 41(3), 234–244. <https://doi.org/10.1016/j.braindev.2018.10.013>

- Osório, A. A. C., & Brunoni, A. R. (2018). Transcranial direct current stimulation in children with autism spectrum disorder: A systematic scoping review. *Developmental Medicine & Child Neurology*. <https://doi.org/10.1111/DMCN.14104>
- Pagnotta, M. F., Zouridakis, G., Lianyang Li, Lizarazu, M., Lallier, M., Molinaro, N., & Carreiras, M. (2015). Low frequency overactivation in dyslexia: Evidence from resting state Magnetoencephalography. *2015 37th Annual International Conference of the IEEE Engineering in Medicine and Biology Society (EMBC)*, 6959–6962. <https://doi.org/10.1109/EMBC.2015.7319993>
- Patton, M. Q. (2014). *Qualitative Research & Evaluation Methods: Integrating Theory and Practice* (4th ed). SAGE Publications.
- Pellicano, E. (2012). The Development of Executive Function in Autism. *Autism Research and Treatment, 2012*, 146132. <https://doi.org/10.1155/2012/146132>
- Qiu, S., Lu, Y., Li, Y., Shi, J., Cui, H., Gu, Y., Li, Y., Zhong, W., Zhu, X., Liu, Y., Cheng, Y., Liu, Y., & Qiao, Y. (2020). Prevalence of autism spectrum disorder in Asia: A systematic review and meta-analysis. *Psychiatry Research*, 284, 112679. <https://doi.org/10.1016/j.psychres.2019.112679>
- Rojas, D. C., & Wilson, L. B. (2014). γ -band abnormalities as markers of autism spectrum disorders. *Biomarkers in Medicine*, 8(3), 353–368. <https://doi.org/10.2217/bmm.14.15>
- Rubinov, M., & Sporns, O. (2010). Complex network measures of brain connectivity: Uses and interpretations. *NeuroImage*, 52(3), 1059–1069. <https://doi.org/10.1016/j.neuroimage.2009.10.003>

- Schneider, B., Heskje, J., Bruss, J., Tranel, D., & Belfi, A. M. (2018). The left temporal pole is a convergence region mediating the relation between names and semantic knowledge for unique entities: Further evidence from a “recognition-from-name” study in neurological patients. *Cortex*, *109*, 14–24. <https://doi.org/10.1016/j.cortex.2018.08.026>
- Sheikhani, A., Behnam, H., Mohammadi, M. R., Noroozian, M., & Mohammadi, M. (2012). Detection of Abnormalities for Diagnosing of Children with Autism Disorders Using of Quantitative Electroencephalography Analysis. *Journal of Medical Systems*, *36*(2), 957–963. <https://doi.org/10.1007/s10916-010-9560-6>
- Sheikhani, A., Behnam, H., Noroozian, M., Mohammadi, M. R., & Mohammadi, M. (2009). Abnormalities of quantitative electroencephalography in children with Asperger disorder in various conditions. *Research in Autism Spectrum Disorders*, *3*(2), 538–546. <https://doi.org/10.1016/j.rasd.2008.11.002>
- Shou, G., Mosconi, M. W., Ethridge, L. E., Sweeney, J. A., & Ding, L. (2018). Resting-state Gamma-band EEG Abnormalities in Autism *. *2018 40th Annual International Conference of the IEEE Engineering in Medicine and Biology Society (EMBC)*, 1915–1918. <https://doi.org/10.1109/EMBC.2018.8512718>
- Sohal, V. S., & Rubenstein, J. L. R. (2019). Excitation-inhibition balance as a framework for investigating mechanisms in neuropsychiatric disorders. *Molecular Psychiatry*, *24*(9), 1248–1257. <https://doi.org/10.1038/s41380-019-0426-0>
- Solomon, O. M., Jr. (1991). PSD computations using Welch’s method. *NASA STI/Recon Technical Report N, 92*, 23584.

- Tadel, F., Bock, E., Niso, G., Mosher, J. C., Cousineau, M., Pantazis, D., Leahy, R. M., & Baillet, S. (2019). MEG/EEG Group Analysis With Brainstorm. *Frontiers in Neuroscience*, *13*, 76. <https://doi.org/10.3389/fnins.2019.00076>
- Toscano, C. V. A., Ferreira, J. P., Gaspar, J. M., & Carvalho, H. M. (2019). Growth and weight status of Brazilian children with autism spectrum disorders: A mixed longitudinal study. *Jornal de Pediatria*, *95*(6), 705–712. <https://doi.org/10.1016/j.jped.2018.06.008>
- Turner Herbert M., I. & Bernard Robert M. (2006). Calculating and Synthesizing Effect Sizes. *Contemporary Issues in Communication Science and Disorders*, *33*(Spring), 42–55. https://doi.org/10.1044/cicsd_33_S_42
- Uddin, L. Q., Nomi, J. S., Hébert-Seropian, B., Ghaziri, J., & Boucher, O. (2017). Structure and Function of the Human Insula: *Journal of Clinical Neurophysiology*, *34*(4), 300–306. <https://doi.org/10.1097/WNP.0000000000000377>
- Uono, S., Sato, W., Kochiyama, T., Kubota, Y., Sawada, R., Yoshimura, S., & Toichi, M. (2017). Time course of gamma-band oscillation associated with face processing in the inferior occipital gyrus and fusiform gyrus: A combined fMRI and MEG study: Neural Basis of Face Processing. *Human Brain Mapping*, *38*(4), 2067–2079. <https://doi.org/10.1002/hbm.23505>
- van Diessen, E., Senders, J., Jansen, F. E., Boersma, M., & Bruining, H. (2015). Increased power of resting-state gamma oscillations in autism spectrum disorder detected by routine electroencephalography. *European Archives of Psychiatry and Clinical Neuroscience*, *265*(6), 537–540. <https://doi.org/10.1007/s00406-014-0527-3>

- Vogan, V. M., Morgan, B. R., Smith, M. L., & Taylor, M. J. (2019). Functional changes during visuo-spatial working memory in autism spectrum disorder: 2-year longitudinal functional magnetic resonance imaging study. *Autism*, 23(3), 639–652. <https://doi.org/10.1177/1362361318766572>
- Ye, A. X., Leung, R. C., Schäfer, C. B., Taylor, M. J., & Doesburg, S. M. (2014). Atypical resting synchrony in autism spectrum disorder: Resting MEG Synchrony in ASD. *Human Brain Mapping*, 35(12), 6049–6066. <https://doi.org/10.1002/hbm.22604>
- Yeh, C., Jones, D. K., Liang, X., Descoteaux, M., & Connelly, A. (2020). Mapping Structural Connectivity Using Diffusion MRI: Challenges and Opportunities. *Journal of Magnetic Resonance Imaging*, jmri.27188. <https://doi.org/10.1002/jmri.27188>
- Yousefi, N., Dadgar, H., & Mohammadi, M. R. (2015). The Validity and Reliability of Autism Behavior Checklist in Iran. *Iranian Journal of Psychiatry, Tehran University of Medical Sciences, Psychiatry and Psychology Research Center*, 10(3), 144–149.
- Zikopoulos, B., & Barbas, H. (2013). Altered neural connectivity in excitatory and inhibitory cortical circuits in autism. *Frontiers in Human Neuroscience*, 7, 609. <https://doi.org/10.3389/fnhum.2013.00609>
- Zoellner, S., Benner, J., Zeidler, B., Seither-Preisler, A., Christiner, M., Seitz, A., Goebel, R., Heinecke, A., Wengenroth, M., Blatow, M., & Schneider, P. (2019). Reduced cortical thickness in Heschl's gyrus as an in vivo marker for human primary auditory cortex. *Human Brain Mapping*, 40(4), 1139–1154. <https://doi.org/10.1002/hbm.24434>

Table 1 Demographic information of subjects

	Gender(male/female)	Ages(year)	ABC(score)	CARS(score)	PEP-3(score)
		Mean(sd)	Mean(sd)	Mean(sd)	Mean(sd)
ASD	8/2	8.70(1.25)	71.5(25.04)	34.3(3.72)	285.70(83.13)
TD	5/5	9.80(1.32)			
<i>t</i>		1.97			
<i>p</i>	0.350	0.07			

sd=standard deviatio

Table 2 Significant inhibition of ROIs

Right hemisphere ROIs	t (permutation test)	z-P SD	p	Effect size (Hedge's g)	Left hemisphere ROIs	t (permutation test)	z-P SD	p
AntObtFrtGyr	-5.76	-4.18	2.87×10^{-5}	-2.42	AntObtFrtGyr	-4.67	-4.27	1.99×10^{-5}
MidObtFrtGyr	-5.41	-4.79	1.66×10^{-6}	-2.21	MidObtFrtGyr	-4.62	-3.77	1.61×10^{-4}
PstObtFrtGyr	-4.63	-3.98	6.98×10^{-5}	-2.00	PstObtFrtGyr	-4.07	-3.60	3.29×10^{-4}
GyrRectus	-4.84	-3.98	6.76×10^{-5}	-1.98	GyrRectus	-4.84	-3.79	1.48×10^{-4}
TsvFrtGyr_Msl	-5.68	-3.90	9.60×10^{-5}	-2.29	TsvFrtGyr_Msl	-5.45	-5.03	4.89×10^{-7}
LatObtFrtGyr_Pst	-5.45	-4.41	1.01×10^{-5}	-2.34	LatObtFrtGyr_Pst	-5.44	-6.64	3.09×10^{-11}
ParsOpcu_Inf	-4.16	-3.88	1.05×10^{-4}	-1.77	ParsOpcu_Inf	-4.48	-6.06	1.34×10^{-9}
ParsOrbitalis	-5.13	-4.37	1.24×10^{-5}	-2.13	ParsOrbitalis	-5.29	-4.39	1.14×10^{-5}
ParsTriagu_Ant	-4.68	-3.86	1.13×10^{-4}	-1.95	ParsTriagu_Ant	-4.43	-5.62	1.97×10^{-8}
ParsTriagu_Mid	-4.81	-5.26	1.41×10^{-7}	-2.02	ParsTriagu_Mid	-3.58	-3.81	1.37×10^{-4}
ParsTriagu_Pst	-3.50	-3.84	1.26×10^{-4}	-1.49	ParsTriagu_Pst	-5.74	-4.17	3.02×10^{-5}
LatObtFrtGyr_Ant	-5.87	-3.59	3.34×10^{-4}	-2.52	MidFrtGyr_Pst	-4.55	-3.80	1.43×10^{-4}
ParsOpcu_Sup	-4.70	-4.42	9.82×10^{-6}	-1.85	PreCentGyr_Inf	-4.80	-3.58	3.40×10^{-4}
InfTepGyr_Ant	-4.49	-4.16	3.18×10^{-5}	-1.91	InfTepGyr_Ant	-5.26	-4.74	2.12×10^{-6}
MidTepGyr_Ant	-4.35	-4.05	5.01×10^{-5}	-1.96	MidTepGyr_Ant	-4.25	-3.58	3.42×10^{-4}
ParaHippoGyr	-3.79	-3.57	3.60×10^{-4}	-1.69	ParaHippoGyr	-4.04	-5.24	1.63×10^{-7}
SupTepGyr_Pst	-4.72	-4.35	1.35×10^{-5}	-2.09	SupTepGyr_Pst	-5.01	-4.95	7.56×10^{-7}

TepPole	-5.03	-4.2	2.22×10^{-4}	-2.18	TepPole	-4.95	-4.9	7.25×10^{-7}
TsvTepGyr	-4.20	-4.1	3.99×10^{-1}	-1.81	TsvTepGyr	-4.20	-4.8	1.22×10^{-5}
					InfTepGyr_Mid	-3.45	-3.5	4.24×10^{-2}
					MidTepGyr_Mid	-4.17	-4.5	4.75×10^{-8}
					MidTepGyr_VenPst	-3.02	-3.6	2.29×10^{-8}
					SupTepGyr_Ant	-4.65	-5.0	5.19×10^{-2}
					SupTepGyr_Mid	-4.97	-4.1	3.20×10^{-6}
					FusiGyr_Ant	-4.01	-4.4	8.68×10^{-5}
Insula_Ant	-3.87	-4.3	1.72×10^{-0}	-1.68	Insula_Ant	-4.40	-4.8	1.23×10^{-5}
Insula_Pst	-4.35	-4.8	1.60×10^{-0}	-1.92				
AnguGyr_Ant	-4.10	-3.9	7.10×10^{-7}	-1.72	AnguGyr_Pst	-4.15	-3.8	1.09×10^{-7}
PreCune_Inf	-3.97	-3.7	2.14×10^{-0}	-1.84				
CingGyr_Ant	-4.93	-4.8	1.59×10^{-0}	-2.02	CingGyr_Ant	-4.95	-5.0	5.47×10^{-1}
SubcallosalGyr	-4.50	-4.9	8.66×10^{-2}	-1.82	SubcallosalGyr	-4.27	-4.2	2.42×10^{-2}
MidOcciGyr_DsoAnt	-4.27	-3.7	1.67×10^{-6}	-1.89	MidOcciGyr_DsoAnt	-3.98	-3.6	3.16×10^{-0}
LingualGyr_Ant	-4.30	-3.8	1.41×10^{-1}	-1.74	Cune_Pst	-4.06	-3.7	2.11×10^{-1}

Table S1 Name, abbreviation and functional systems of ROIs

Name	Abbreviation	Function System
left anterior angular gyrus	AnguGyr_Ant_L	HOC
right anterior angular gyrus	AnguGyr_Ant_R	HOC
left middle angular gyrus	AnguGyr_Mid_L	HOC
right middle angular gyrus	AnguGyr_Mid_R	HOC
left posterior angular gyrus	AnguGyr_Pst_L	HOC
right posterior angular gyrus	AnguGyr_Pst_R	HOC
left anterior orbitofrontal gyrus	AntObtFrtGyr_L	HOC
right anterior orbitofrontal gyrus	AntObtFrtGyr_R	HOC
left anterior cingulate gyrus	CingGyr_Ant_L	HOC
right anterior cingulate gyrus	CingGyr_Ant_R	HOC
left middle cingulate gyrus	CingGyr_Mid_L	MDM
right middle cingulate gyrus	CingGyr_Mid_R	MDM
left posterior cingulate gyrus	CingGyr_Pst_L	MDM
right posterior cingulate gyrus	CingGyr_Pst_R	MDM
left anterior cuneus	Cune_Ant_L	SAA
right anterior cuneus	Cune_Ant_R	SAA
left posterior cuneus	Cune_Pst_L	SAA
right posterior cuneus	Cune_Pst_R	SAA
left anterior fusiform gyrus	FusiGyr_Ant_L	SAA
right anterior fusiform gyrus	FusiGyr_Ant_R	SAA
left posterior fusiform gyrus	FusiGyr_Pst_L	SAA
right posterior fusiform gyrus	FusiGyr_Pst_R	SAA
left gyrus rectus	GyrRectus_L	HOC
right gyrus rectus	GyrRectus_R	HOC
left anterior inferior occipital gyrus	InfOcciGyr_Ant_L	SAA
right anterior inferior occipital gyrus	InfOcciGyr_Ant_R	SAA
left dorsoposterior inferior occipital gyrus	InfOcciGyr_DsoPst_L	SAA
right dorsoposterior inferior occipital gyrus	InfOcciGyr_DsoPst_R	SAA
left ventroposterior inferior occipital gyrus	InfOcciGyr_VenPst_L	SAA
right ventroposterior inferior occipital gyrus	InfOcciGyr_VenPst_R	SAA
left anterior inferior temporal gyrus	InfTepGyr_Ant_L	SAA
right anterior inferior temporal gyrus	InfTepGyr_Ant_R	SAA
left middle inferior temporal gyrus	InfTepGyr_Mid_L	SAA
right middle inferior temporal gyrus	InfTepGyr_Mid_R	SAA
left posterior inferior temporal gyrus	InfTepGyr_Pst_L	SAA
right posterior inferior temporal gyrus	InfTepGyr_Pst_R	SAA
left anterior insula	Insula_Ant_L	HOC
right anterior insula	Insula_Ant_R	HOC
left posterior insula	Insula_Pst_L	HOC
right posterior insula	Insula_Pst_R	HOC
left anterior lateral orbitofrontal gyrus	LatObtFrtGyr_Ant_L	HOC
right anterior lateral orbitofrontal gyrus	LatObtFrtGyr_Ant_R	HOC
left posterior lateral orbitofrontal gyrus	LatObtFrtGyr_Pst_L	HOC
right posterior lateral orbitofrontal gyrus	LatObtFrtGyr_Pst_R	HOC
left anterior lingual gyrus	LingualGyr_Ant_L	SAA

Name	Abbreviation	Function System
right anterior lingual gyrus	LingualGyr_Ant_R	SAA
left posterior lingual gyrus	LingualGyr_Pst_L	SAA
right posterior lingual gyrus	LingualGyr_Pst_R	SAA
left anterior middle frontal gyrus	MidFrtGyr_Ant_L	HOC
right anterior middle frontal gyrus	MidFrtGyr_Ant_R	HOC
left posterior middle frontal gyrus	MidFrtGyr_Pst_L	HOC
right posterior middle frontal gyrus	MidFrtGyr_Pst_R	HOC
left dorsoanterior middle occipital gyrus	MidOcciGyr_DsoAnt_L	SAA
right dorsoanterior middle occipital gyrus	MidOcciGyr_DsoAnt_R	SAA
left posterior middle occipital gyrus	MidOcciGyr_Pst_L	SAA
right posterior middle occipital gyrus	MidOcciGyr_Pst_R	SAA
left ventroanterior middle occipital gyrus	MidOcciGyr_VenAnt_L	SAA
right ventroanterior middle occipital gyrus	MidOcciGyr_VenAnt_R	SAA
left middle orbitofrontal gyrus	MidObtFrtGyr_L	HOC
right middle orbitofrontal gyrus	MidObtFrtGyr_R	HOC
left anterior middle temporal gyrus	MidTepGyr_Ant_L	SAA
right anterior middle temporal gyrus	MidTepGyr_Ant_R	SAA
left dorsoposterior middle temporal gyrus	MidTepGyr_DsoPst_L	SAA
right dorsoposterior middle temporal gyrus	MidTepGyr_DsoPst_R	SAA
left middle middle temporal gyrus	MidTepGyr_Mid_L	SAA
right middle middle temporal gyrus	MidTepGyr_Mid_R	SAA
left ventroposterior middle temporal gyrus	MidTepGyr_VenPst_L	SAA
right ventroposterior middle temporal gyrus	MidTepGyr_VenPst_R	SAA
left paracentral lobule	ParaCentLob_L	SAA
right paracentral lobule	ParaCentLob_R	SAA
left parahippocampal gyrus	ParaHippoGyr_L	SAA
right parahippocampal gyrus	ParaHippoGyr_R	SAA
left inferior pars opercularis	ParsOpcu_Inf_L	HOC
right inferior pars opercularis	ParsOpcu_Inf_R	HOC
left superior pars opercularis	ParsOpcu_Sup_L	HOC
right superior pars opercularis	ParsOpcu_Sup_R	HOC
left pars orbitalis	ParsOrbitalis_L	HOC
right pars orbitalis	ParsOrbitalis_R	HOC
left anterior pars triangularis	ParsTriagu_Ant_L	HOC
right anterior pars triangularis	ParsTriagu_Ant_R	HOC
left middle pars triangularis	ParsTriagu_Mid_L	HOC
right middle pars triangularis	ParsTriagu_Mid_R	HOC
left posterior pars triangularis	ParsTriagu_Pst_L	HOC
right posterior pars triangularis	ParsTriagu_Pst_R	HOC
left inferior postcentral gyrus	PostCentGyr_Inf_L	SAA
right inferior postcentral gyrus	PostCentGyr_Inf_R	SAA
left superior postcentral gyrus	PostCentGyr_Sup_L	SAA
right superior postcentral gyrus	PostCentGyr_Sup_R	SAA
left posterior orbitofrontal gyrus	PstObtFrtGyr_L	HOC
right posterior orbitofrontal gyrus	PstObtFrtGyr_R	HOC

Name	Abbreviation	Function System
left inferior precentral gyrus	PreCentGyr_Inf_L	SAA
right inferior precentral gyrus	PreCentGyr_Inf_R	SAA
left superior precentral gyrus	PreCentGyr_Sup_L	SAA
right superior precentral gyrus	PreCentGyr_Sup_R	SAA
left inferior precuneus	PreCune_Inf_L	MDM
right inferior precuneus	PreCune_Inf_R	MDM
left superior precuneus	PreCune_Sup_L	MDM
right superior precuneus	PreCune_Sup_R	MDM
left subcallosal gyrus	SubcallosalGyr_L	MDM
right subcallosal gyrus	SubcallosalGyr_R	MDM
left anterior superior frontal gyrus	SupFrtGyr_Ant_L	MDM
right anterior superior frontal gyrus	SupFrtGyr_Ant_R	MDM
left posterior superior frontal gyrus	SupFrtGyr_Pst_L	MDM
right posterior superior frontal gyrus	SupFrtGyr_Pst_R	MDM
left inferior superior occipital gyrus	SupOcciGyr_Inf_L	SAA
right inferior superior occipital gyrus	SupOcciGyr_Inf_R	SAA
left superior superior occipital gyrus	SupOcciGyr_Sup_L	SAA
right superior superior occipital gyrus	SupOcciGyr_Sup_R	SAA
left anterior superior parietal gyrus	SupPariGyr_Ant_L	HOC
right anterior superior parietal gyrus	SupPariGyr_Ant_R	HOC
left posterior superior parietal gyrus	SupPariGyr_Pst_L	HOC
right posterior superior parietal gyrus	SupPariGyr_Pst_R	HOC
left anterior superior temporal gyrus	SupTepGyr_Ant_L	SAA
right anterior superior temporal gyrus	SupTepGyr_Ant_R	SAA
left middle superior temporal gyrus	SupTepGyr_Mid_L	SAA
right middle superior temporal gyrus	SupTepGyr_Mid_R	SAA
left posterior superior temporal gyrus	SupTepGyr_Pst_L	SAA
right posterior superior temporal gyrus	SupTepGyr_Pst_R	SAA
left anterior supramarginal gyrus	SprmarGyr_Ant_L	HOC
right anterior supramarginal gyrus	SprmarGyr_Ant_R	HOC
left posterior supramarginal gyrus	SprmarGyr_Pst_L	HOC
right posterior supramarginal gyrus	SprmarGyr_Pst_R	HOC
left temporal pole	TepPole_L	SAA
right temporal pole	TepPole_R	SAA
left lateral transverse frontal gyrus	TsvFrtGyr_Lat_L	HOC
right lateral transverse frontal gyrus	TsvFrtGyr_Lat_R	HOC
left mesial transverse frontal gyrus	TsvFrtGyr_Msl_L	HOC
right mesial transverse frontal gyrus	TsvFrtGyr_Msl_R	HOC
left transverse temporal gyrus	TsvTepGyr_L	SAA
right transverse temporal gyrus	TsvTepGyr_R	SAA

HOC: Higher Order Cognitive; MDM: Medial Default Mode; SAA: Sensory and Association System.

Table S2 Function of ROIs with significant mPTEs differences

ROIs	Function	References
left anterior orbitofrontal gyrus	decision-making	(Du et al., 2020; Fatahi et al., 2020; Premkumar et al., 2015; Ouellet et al., 2015)
left anterior lateral orbitofrontal gyrus	decision-making	(Du et al., 2020; Fatahi et al., 2020; Premkumar et al., 2015; Ouellet et al., 2015; Kobayakawa et al., 2017)
left temporal pole	semantic processing	(Schneider et al., 2018; Tsapkini et al., 2011; Binder et al., 2020)
left lateral transverse frontal gyrus	Auditory-attention	(Michalka et al., 2015; Noyce et al., 2017)
left anterior angular gyrus	semantic processing	(Bemis and Pylkkänen, 2013; Matchin et al., 2019)
left anterior inferior occipital gyrus	face processing	(Uono et al., 2017; Solomon-Harris et al., 2016; Sato et al., 2014)
left parahippocampal	memory	(Karanian and Slotnick, 2017; Jacobs et al., 2015; Li et al., 2016)

References of Table S2

- Bemis, D. K., & Pylkkänen, L. (2013). Basic Linguistic Composition Recruits the Left Anterior Temporal Lobe and Left Angular Gyrus During Both Listening and Reading. *Cerebral Cortex*, 23, 1859–1873. <https://doi.org/10.1093/cercor/bhs170>
- Binder, J. R., Tong, J., Pillay, S. B., Conant, L. L., Humphries, C. J., Raghavan, M., Mueller, W. M., Busch, R. M., Allen, L., Gross, W. L., Anderson, C. T., Carlson, C. E., Lowe, M. J., Langfitt, J. T., Tivarus, M. E., Drane, D. L., Loring, D. W., Jacobs, M., Morgan, V. L., ... Swanson, S. J. (2020). Temporal lobe regions essential for preserved picture naming after left temporal epilepsy surgery. *Epilepsia*, 61(9), 1939–1948. <https://doi.org/10.1111/epi.16643>
- Boylan, C., Trueswell, J. C., & Thompson-Schill, S. L. (2015). Compositionality and the angular gyrus: A multi-voxel similarity analysis of the semantic composition of nouns and verbs. *Neuropsychologia*, 78, 130–141. <https://doi.org/10.1016/j.neuropsychologia.2015.10.007>

- Du, J., Rolls, E. T., Cheng, W., Li, Y., Gong, W., Qiu, J., & Feng, J. (2020). Functional connectivity of the orbitofrontal cortex, anterior cingulate cortex, and inferior frontal gyrus in humans. *CORTEX*, *123*, 185–199. <https://doi.org/10.1016/j.cortex.2019.10.012>
- Fatahi, Z., Ghorbani, A., Ismail Zibaii, M., & Haghparast, A. (2020). Neural synchronization between the anterior cingulate and orbitofrontal cortices during effort-based decision making. *Neurobiology of Learning and Memory*, *175*, 107320. <https://doi.org/10.1016/j.nlm.2020.107320>
- Jacobs, H. I. L., Wiese, S., van de Ven, V., Gronenschild, E. H. B. M., Verhey, F. R. J., & Matthews, P. M. (2015). Relevance of parahippocampal-locus coeruleus connectivity to memory in early dementia. *Neurobiology of Aging*, *36*(2), 618–626. <https://doi.org/10.1016/j.neurobiolaging.2014.10.041>
- Karanian, J. M., & Slotnick, S. D. (2017). False memory for context and true memory for context similarly activate the parahippocampal cortex. *Cortex*, *91*, 79–88. <https://doi.org/10.1016/j.cortex.2017.02.007>
- Kobayakawa, M., Tsuruya, N., & Kawamura, M. (2017). Decision-making performance in Parkinson's disease correlates with lateral orbitofrontal volume. *Journal of the Neurological Sciences*, *372*, 232–238. <https://doi.org/10.1016/j.jns.2016.11.046>
- Li, M., Lu, S., & Zhong, N. (2016). The Parahippocampal Cortex Mediates Contextual Associative Memory: Evidence from an fMRI Study. *BioMed Research International*, *2016*, 1–11. <https://doi.org/10.1155/2016/9860604>
- Matchin, W., Liao, C.-H., Gaston, P., & Lau, E. (2019). Same words, different structures_ an fMRI investigation of argument relations and the angular gyrus. *Neuropsychologia*, *125*, 116–128. <https://doi.org/10.1016/j.neuropsychologia.2019.01.019>
- Michalka, S. W., Kong, L., Rosen, M. L., Shinn-Cunningham, B. G., & Somers, D. C. (2015). Short-Term Memory for Space and Time Flexibly Recruit Complementary Sensory-Biased Frontal Lobe Attention Networks. *Neuron*, *87*(4), 882–892. <https://doi.org/10.1016/j.neuron.2015.07.028>
- Noyce, A. L., Cestero, N., Michalka, S. W., Shinn-Cunningham, B. G., & Somers, D. C. (2017). Sensory-biased and multiple-demand processing in human lateral frontal cortex. *The Journal of Neuroscience*, *37*(36), 8755–8766. <https://doi.org/10.1523/JNEUROSCI.0660-17.2017>
- Ouellet, J., McGirr, A., Van den Eynde, F., Jollant, F., Lepage, M., & Berlim, M. T. (2015). Enhancing decision-making and cognitive impulse control with transcranial direct current stimulation (tDCS) applied over the orbitofrontal cortex (OFC): A randomized and

sham-controlled exploratory study. *Journal of Psychiatric Research*, 69, 27–34.

<https://doi.org/10.1016/j.jpsychires.2015.07.018>

Premkumar, P., Fannon, D., Sapara, A., Peters, E. R., Anilkumar, A. P., Simmons, A., Kuipers, E., & Kumari, V. (2015). Orbitofrontal cortex, emotional decision-making and response to cognitive behavioural therapy for psychosis. *Psychiatry Research: Neuroimaging*, 231(3), 298–307.

<https://doi.org/10.1016/j.psychres.2015.01.013>

Sato, W., Kochiyama, T., Uono, S., Matsuda, K., Usui, K., Inoue, Y., & Toichi, M. (2014). Rapid, high-frequency, and theta-coupled gamma oscillations in the inferior occipital gyrus during face processing. *Cortex*, 60, 52–68. <https://doi.org/10.1016/j.cortex.2014.02.024>

Schneider, B., Heskje, J., Bruss, J., Tranel, D., & Belfi, A. M. (2018). The left temporal pole is a convergence region mediating the relation between names and semantic knowledge for unique entities: Further evidence from a “recognition-from-name” study in neurological patients. *Cortex*, 109, 14–24. <https://doi.org/10.1016/j.cortex.2018.08.026>

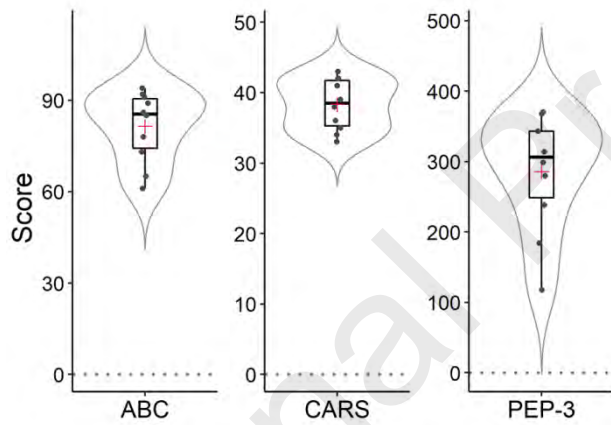
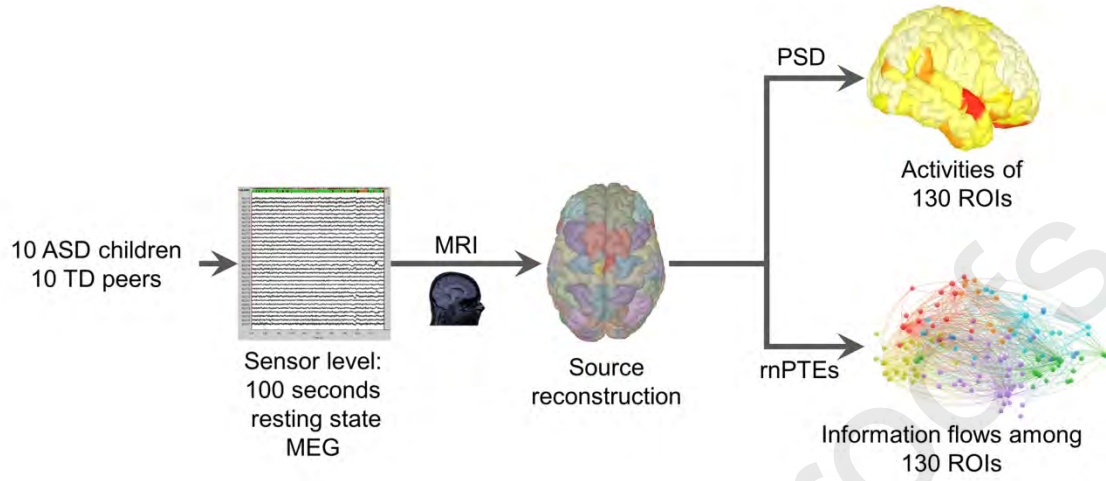
Solomon-Harris, L. M., Rafique, S. A., & Steeves, J. K. E. (2016). Consecutive TMS-fMRI Reveals Remote Effects of Neural Noise to the “Occipital Face Area”. *Brain Research*, 1650, 134–141.

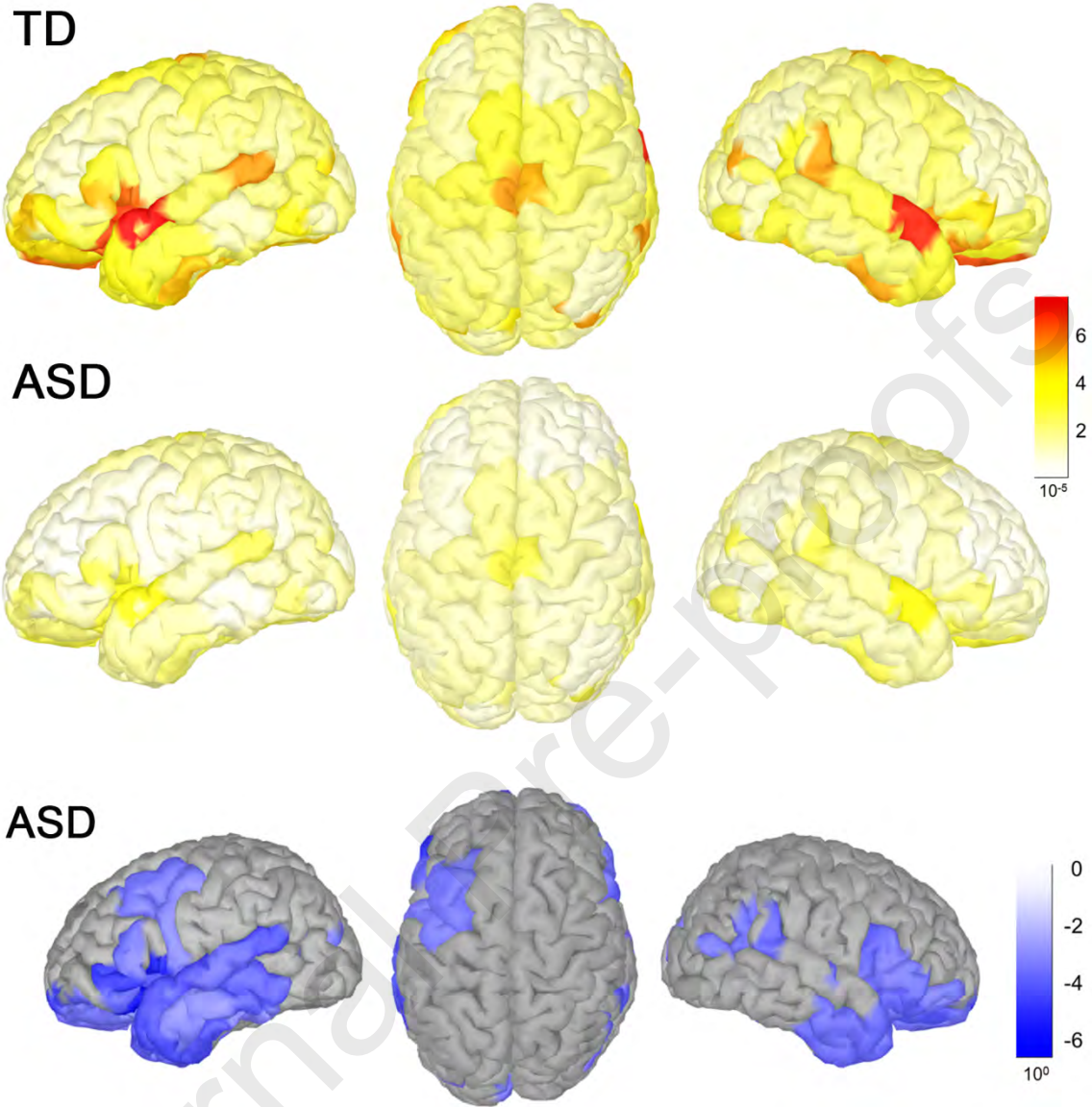
<https://doi.org/10.1016/j.brainres.2016.08.043>

Tsapkini, K., Frangakis, C. E., & Hillis, A. E. (2011). The function of the left anterior temporal pole: Evidence from acute stroke and infarct volume. *Brain*, 134, 3094–3105.

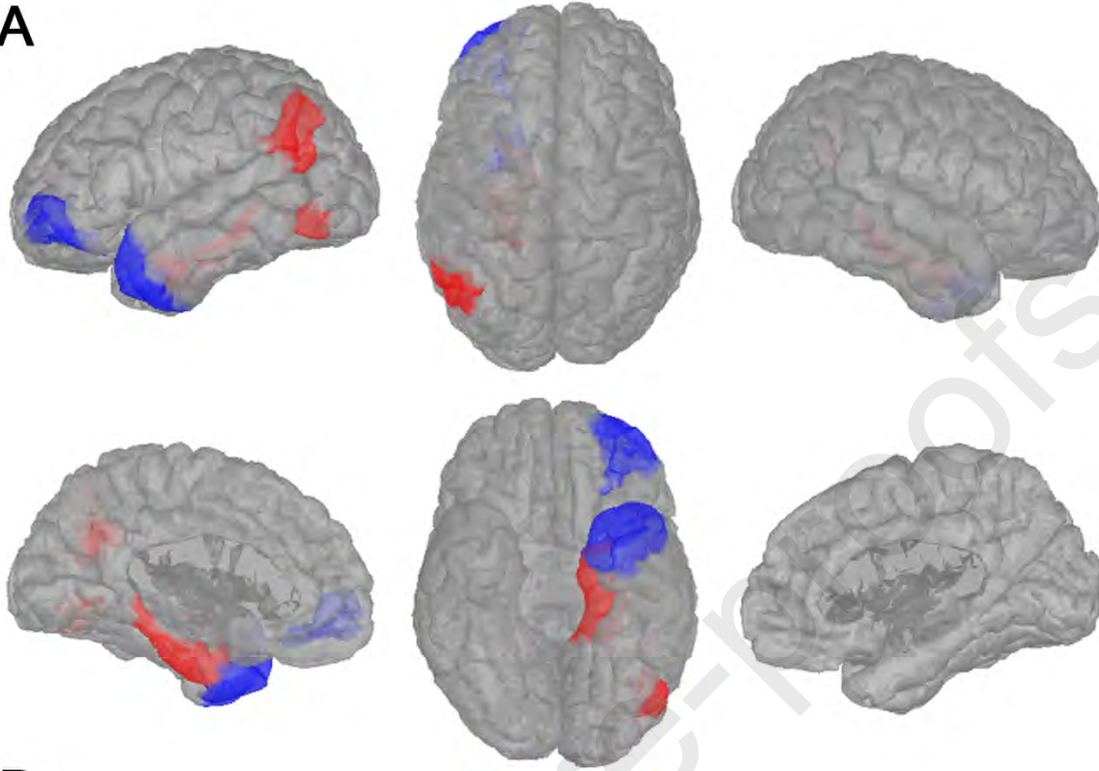
<https://doi.org/10.1093/brain/awr050>

Uono, S., Sato, W., Kochiyama, T., Kubota, Y., Sawada, R., Yoshimura, S., & Toichi, M. (2017). Time course of gamma-band oscillation associated with face processing in the inferior occipital gyrus and fusiform gyrus: A combined fMRI and MEG study: Neural Basis of Face Processing. *Human Brain Mapping*, 38(4), 2067–2079. <https://doi.org/10.1002/hbm.23505>

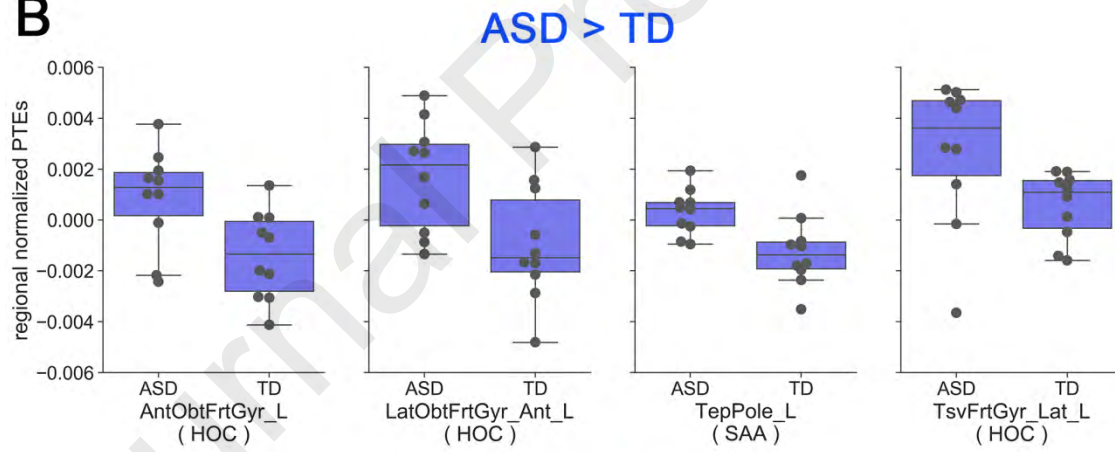




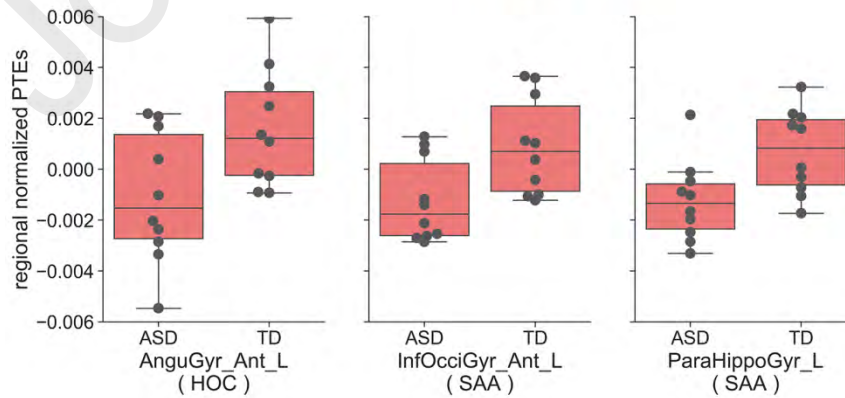
A

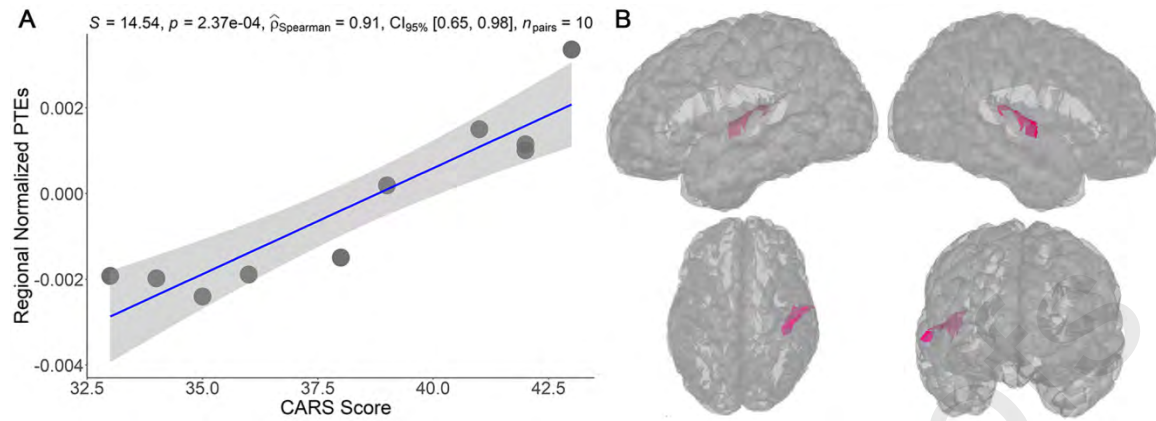


B



ASD < TD





Highlights

- Brain activity is suppressed at the gamma-band level in children with autism.
- Distribution and intensity of the information flow in autistic children's brain network is aberrant.
- Connectivity of right Heschl's gyrus is associated with clinical manifestations in children with autism.